Penerbit Akademia Baru

Journal of Research in Nanoscience and Nanotechnology

Journal homepage:
http://akademiabaru.com/submit/index.php/jrnn/index
ISSN: 2773-6180

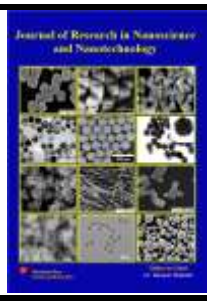

Feasibility of chitosan-based nanoparticles for gene delivery compared to lipofectamine as a common transfection reagent

Sanaz Bagheri [1], Hassan Moeini [2] and Kamyar Shameli [1,*]

[1] School of Medicine, Institute of Virology, Technical University of Munich, 81675 Munich, Germany
[2] Iguana Biotechnology GmbH, 80331 Munich, Germany
* Correspondence: kamyar.shameli@tum.de
https://doi.org/10.37934/jrnn.13.1.122

ABSTRACT

This study optimizes chitosan nanoparticles (Cts-NPs) for nucleic acid delivery, examining the impact of varying tripolyphosphate (TPP) to Cts molar ratios on ζ-potential, size, and binding efficiency. The ζ-potential of the Cts solution decreased from +38.85 mV to -0.12 mV as TPP increased. Samples S3 and S4, with ζ-potentials of +28.76 and +13.11 mV, were optimal due to their efficiency and nucleic acid binding capability. UV-visible spectroscopy confirmed DNA binding to Cts-NPs, and FTIR analysis revealed successful DNA incorporation through electrostatic interactions and cross-linking, crucial for stability and controlled release. TEM analysis showed S3 had an average NP size of 8.79 ± 2.23 nm, indicating uniform, spherical particles. GFP expression in HepG2 and HEK293 cells assessed transfection efficiency, comparing Cts-DNA NPs with Lipofectamine 2000, which achieved over 70% efficiency versus less than 10% for Cts-DNA NPs. Comparing Lipofectamine 3000, Transfex, and Fugene, Lipofectamine 3000 showed the highest efficiency (over 70%) but high cytotoxicity, especially in HepG2 cells. Transfex showed moderate efficiency (~40%) and cytotoxicity, while Fugene had the lowest efficiency (<10%) but minimal cytotoxicity. In conclusion, S3 and S4 Cts-NPs balance size, charge, and efficiency for nucleic acid delivery, while Lipofectamine 3000 is highly effective but cytotoxic. Balancing efficiency and cytotoxicity are crucial for gene delivery systems.

Keywords:
Chitosan nanoparticles, DNA delivery, Lipofectamine, Transfection reagents, Cytotoxicity

Received: 27 May 2024 **Revised: 20 Jun. 2024** **Accepted: 25 Jul. 2024** **Published: 30 Aug. 2024**

1. Introduction

Chitosan (Cts) is a useful biomaterial derived from deacetylation of chitin (poly(β-1,4-Nacetyl-D-glucose-2-amine)), which is one of the most abundant natural polysaccharides, found in the cell walls of microorganisms such as yeasts or other fungi, in the exoskeletons of crustaceans and insects. Physical and chemical properties of Cts depend mainly on its molecular weight and degree of deacetylation. Cts is recognized as a biocompatible, biodegradable, bio adhesive, and nontoxic material [1]. As a natural biocompatible polymer, Cts has been extensively investigated in pharmaceutical research and in industry for drug delivery and as biomedical material [2, 3]. During

the last two decades Cts has been investigated as a hydrophilic material for nanoparticles (NPs) because of its accepted mucoadhesive and ability to enhance the penetration of large molecules across mucosal surface [4, 5] (Figure 1).

Cts-NPs hold marked mucoadhesive properties that have been related to the combination of the particle size and the particle superficial charge. It has the ability to control the drug release rate, lengthen the duration of therapeutic effectiveness, and deliver the drug to precise sites in the body. Under acidic conditions, Cts can be dissolved in water after amino protonation to confer high positive charge density. These positive charges qualify Cts both to interact with polyanion to form complexes, then gels as well as adhere to the mucosal membrane which improves the absorption of the drugs across cellular barriers [6, 7].

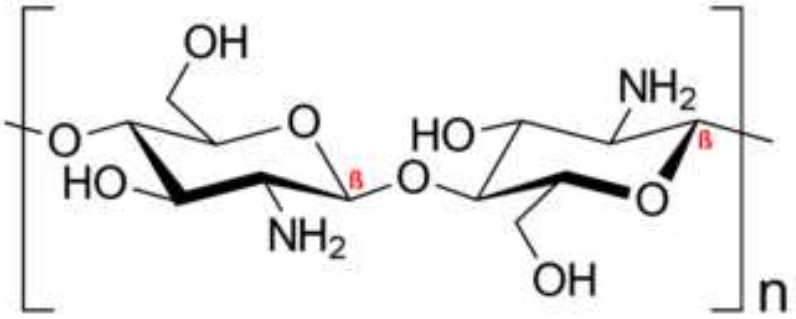

Fig. 1. Illustration of Cts's molecular structure, a biopolymer from chitin with repeating β-(1→4)-linked D-glucosamine units. Cts is widely used in biomedical applications for its biocompatibility and biodegradability

Peptides, proteins, gens and antigens have become the drugs of choice for treatment of various diseases as a result of their assured selectivity and their ability to provide effective and fascinating action [8]. However, they are poorly absorbed after oral administration because of their poor liability to enzymatic degradation and their low permeability across the intestinal epithelium. In addition, their rapid clearance from the blood stream and low permeability across some biological barriers such as the blood-brain barrier, limit its applications. Recently, the hydrophilic NPs such as Cts-NPs have received considerable attention to deliver such drugs by intravenous, oral, and mucosal administration [9]. Probably, the most standard way to produce Cts-NPs is through ionotropic gelation that is physical crosslinking, of Cts with sodium Tripolyphosphate (TPP). TPP is a small ion with a triple negative charge throughout the physiologically acceptable pH range [10-12]. Non-toxicity and quick gelling ability of TPP are the important properties that make it a satisfactory cross-linker for ionic gelation of Cts [13] (Figure 2). It was reported that at concentrations below 2 mg/mL and 0.4 mg/mL respectively for TPP and Cts, should be used, in order to avoid the formation of large aggregates.

Figure 2 illustrated that Cts-NPs cross-linked with TPP predominantly formed NPs where Cts chains were interconnected via cross-linker agents. These polysaccharide-based NPs possessed cationic charged surfaces, facilitating interactions such as van der Waals forces and/or covalent bonding with anionic charged proteins or genes. This electrostatic interaction was crucial for their function in various biomedical applications, including drug delivery and gene therapy [14]. The cationic charge of Cts enabled it to bind effectively with anionic charged biomolecules, enhancing the stability and efficacy of loaded payloads within the NPs. Moreover, the ability to form bonds with proteins or genes suggested versatility in targeting specific cells or tissues, potentially optimizing

therapeutic outcomes. Understanding these interactions was fundamental for designing and optimizing NP-based delivery systems, ensuring efficient and targeted delivery of therapeutic agents while minimizing off-target effects. Future research will be focused on further elucidating the precise mechanisms and expanding the applications of these bio-NPs in biomedical sciences and clinical settings. The mass ratio of cross-linked Cts-NPs between Cts and TPP should not have been large; larger Cts-TPP ratios yielded particles with larger size and zeta potential [11, 14]. Zhang et al. [15] developed some of the initial studies [16-18], investigating the effect of Cts fractional precipitation and deacetylation as means to increase its TPP-binding efficiency. Recently, Nasti et al. systematically optimized the preparative process of cross-linked Cts-NPs [19].

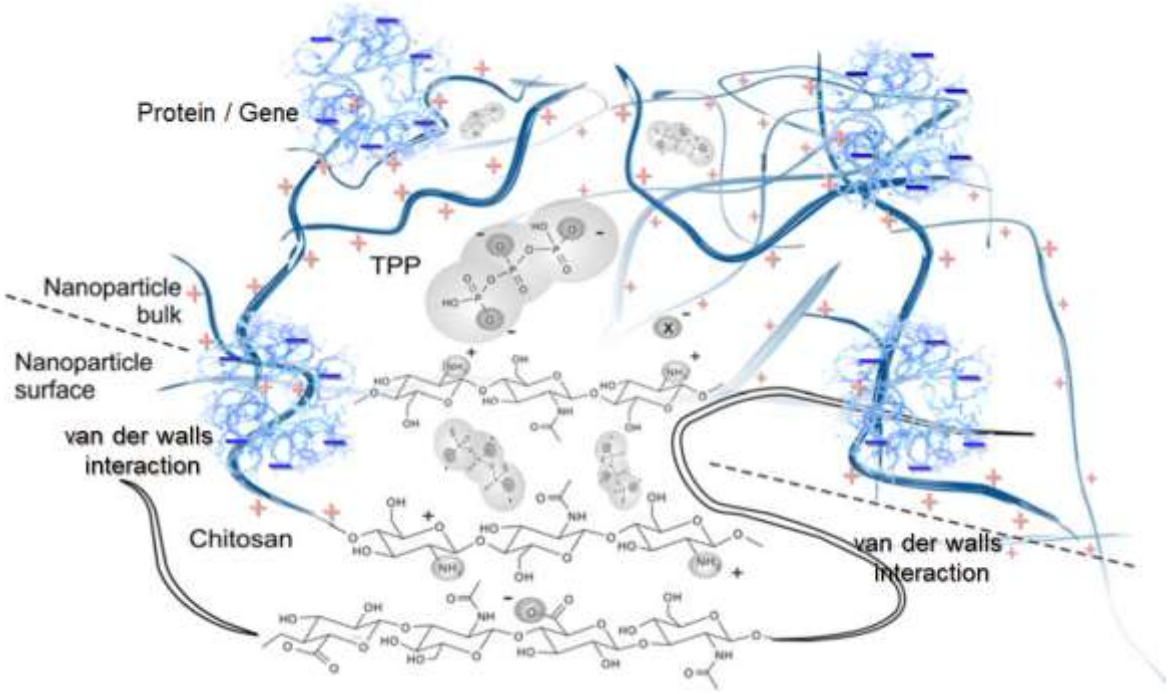

Fig. 2. Crosslinked Cts-NPs using TPP as a cross-bridge polymer chain facilitate self-binding with anionic proteins/genes on the cationic chitosan surface through van der walls interaction [14]

Cts-NPs exhibit a unique integration effect due to their dual molecular characteristics of hydrophobicity and hydrophilicity. This property makes them versatile for various biomedical applications. Their inherent biological properties include non-toxicity, antimicrobial activity, mucoadhesivity, and hemocompatibility, which contribute significantly to their appeal in pharmaceutical and biomedical fields (Figure 3). The hydrophobic and hydrophilic nature of Cts-NPs allows them to interact with both water-soluble and lipid-soluble substances, facilitating the encapsulation and delivery of diverse therapeutic agents such as drugs, proteins, and genes. Their biocompatibility ensures minimal adverse effects when administered in vivo, making them suitable candidates for drug delivery systems [20]. Additionally, their antimicrobial properties enable applications in wound dressings and infection control. Furthermore, Cts-NPs exhibit mucoadhesive properties, meaning they can adhere to mucosal surfaces, prolonging drug residence time and enhancing absorption. This property is advantageous for localized drug delivery to specific tissues or organs. Their hemocompatibility ensures compatibility with blood components, minimizing risks of clotting or immune reactions during systemic administration [20]. Overall, the multifaceted properties of Cts-NPs position them as promising candidates for advancing biomedical technologies,

particularly in targeted drug delivery, wound healing, and therapeutic interventions that require safe and effective nanoparticle-based systems.

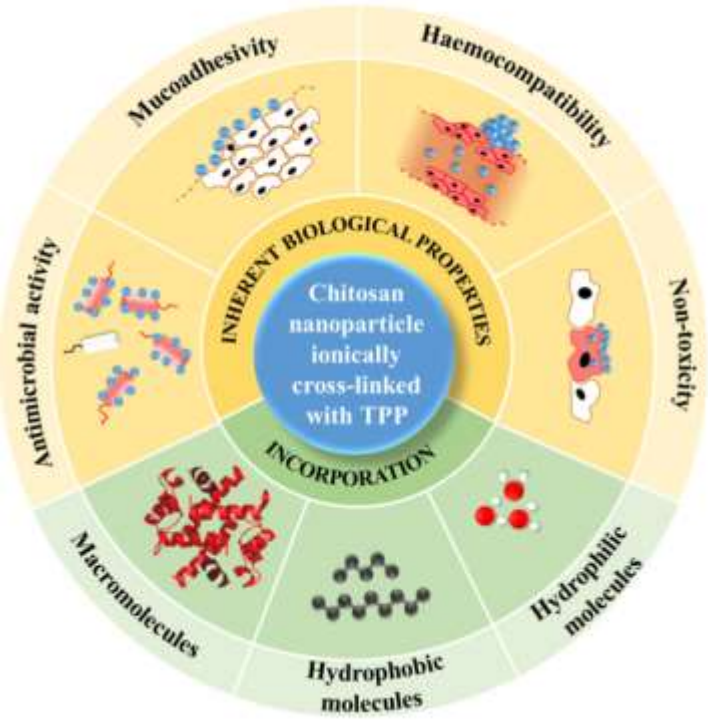

Fig. 3. Characteristics of cross-linked Cts-NPs considered in this report include their inherent biological properties and their ability to incorporate various bioactive species [20]

Designing effective Cts-based NPs for gene delivery hinges on optimizing several critical factors that collectively determine their functionality and performance. The molecular weight of Cts is a pivotal aspect, as lower molecular weights enhance drug loading capacity but may compromise NPs stability, whereas higher molecular weights improve stability but can reduce loading capacity [21]. Another vital factor is the degree of deacetylation (DDA), which affects the surface charge of Cts-NPs; higher DDA results in a more positive charge, facilitating better electrostatic interactions with negatively charged nucleic acids but potentially increasing cytotoxicity [22]. The preparation method, whether ionic gelation, emulsification-solvent evaporation, or co-precipitation, plays a significant role in defining particle size, morphology, and gene encapsulation efficiency [23]. Moreover, surface functionalization with specific ligands or targeting moieties enables targeted delivery to particular cell types, significantly enhancing therapeutic efficacy [24]. Additionally, such functionalization can introduce responsiveness to environmental stimuli like pH or temperature, enabling controlled release of the gene only under desired conditions, thus improving therapeutic outcomes [25]. Furthermore, modifying the surface with hydrophilic polymers can enhance biocompatibility and prolong circulation time, reducing cytotoxicity [26]. Collectively, these considerations are essential for developing Cts-NPs that are highly effective for gene delivery applications.

HepG2 cells, a human hepatocellular carcinoma cell line, are a mainstay in virology research, particularly for studies involving viruses that target the liver. Their widespread use stems from several key advantages [27]. HepG2 cells are derived from human liver tissue. This human origin provides a more relevant cellular environment for studying human viruses compared to using cell

lines from other species. Viruses often exhibit host-specific interactions, and using human cells allows researchers to observe these interactions more closely mimicking the natural infection process [27].

HepG2 cells demonstrate susceptibility to a broad range of viruses, including major human liver pathogens like hepatitis B virus (HBV) and hepatitis C virus (HCV) [28]. This versatility makes them a valuable tool for studying diverse viruses and their interactions with human liver cells. Researchers can utilize HepG2 cells to investigate viral entry mechanisms, replication cycles, and pathogenic effects on liver cells. HepG2 cells are well-characterized. Extensive research has established a vast knowledge base about their properties and behavior [29]. This well-defined nature allows researchers to interpret experimental results with greater confidence, attributing observed effects specifically to the virus under study rather than unfamiliar properties of the cell line. HepG2 cells are relatively easy to grow and maintain in culture [30]. This characteristic is crucial for large-scale experiments and routine viral propagation. The ability to consistently produce large quantities of cells facilitates efficient research workflows and enables studies requiring multiple replicates or high cell numbers. While not perfect, HepG2 cells do express some functionalities of mature liver cells, such as the production of certain proteins involved in metabolism and detoxification [31]. This ability can be beneficial for studying how viruses affect these vital liver processes. HepG2 cells offer a valuable combination of human origin, broad viral susceptibility, well-characterized properties, ease of use, and partial liver functionality. These advantages make them a versatile and widely used tool for researchers investigating viruses that target the liver. Transfection reagents are critical tools in molecular biology used to introduce nucleic acids such as DNA or RNA into eukaryotic cells. These reagents facilitate the delivery of genetic material into the cell by overcoming the cell membrane barrier, allowing for the study of gene function, protein expression, and genetic modification. Common transfection reagents include liposomes, calcium phosphate, and polymer-based systems. Liposomes, for example, are lipid-based vesicles that encapsulate nucleic acids and fuse with cell membranes to deliver their cargo. Polymer-based reagents often utilize cationic polymers that form complexes with negatively charged nucleic acids, facilitating their uptake by cells [32]. While both transfection reagents and Cts-NPs serve the fundamental purpose of gene delivery, they exhibit distinct differences in their composition, mechanisms of action, and applications. Traditional transfection reagents, particularly liposomes, are synthesized through chemical processes and often require optimization for each cell type and experimental condition. These reagents can achieve high transfection efficiency but may also induce cytotoxicity and immune responses [33]. In contrast, Cts-NPs are naturally derived and generally exhibit lower cytotoxicity and immunogenicity. Their biocompatibility and ability to protect nucleic acids from enzymatic degradation make them attractive for in vivo applications. Furthermore, Cts-NPs can be modified chemically to enhance their transfection efficiency and target specificity, making them versatile tools for gene therapy and vaccination [34]. Despite these differences, there are similarities in their applications and challenges. Both systems require optimization to achieve efficient gene delivery while minimizing adverse effects. Additionally, both are subject to endosomal entrapment, necessitating the use of strategies to enhance endosomal escape and improve transfection outcomes [35]. Transfection reagents and Cts-NPs represent complementary approaches to gene delivery, each with unique advantages and limitations. The choice between these systems depends on the specific requirements of the experimental or therapeutic application, including considerations of efficiency, toxicity, and biocompatibility. Ongoing research and development in this field aim to overcome existing challenges and enhance the efficacy of these gene delivery systems. Lipofectamine 3000 (Thermo Fisher Scientific), a cationic lipid-based reagent forms liposomes that encapsulate and deliver DNA or siRNA into cells. It is widely used for various cell types due to its high transfection efficiency [36]. However, Lipofectamine can be expensive and demonstrate cytotoxicity in some cell lines [37].

FuGENE (Promega) is another popular cationic polymer-based reagent, also forms complexes with DNA or siRNA for cellular delivery. It offers good transfection efficiency but can be less versatile across different cell types compared to Lipofectamine [38]. However, similar to lipofectamine, FuGENE can be costly and potentially cytotoxic. Transfex (Bio-Rad), a cationic polymer transfection reagent functions similarly to FuGENE, but it may be less efficient for some cell lines. Transfex generally offers a lower price point compared to lipofectamine and FuGENE, but its cytotoxicity profile can vary depending on the cell type [39]. While traditional transfection reagents like lipofectamine, FuGENE, and transfex have been instrumental in viral research, Cts-NPs offer a promising alternative with improved biocompatibility, targeted delivery, and cost-effectiveness.

As research progresses, Cts-NPs have the potential to become a powerful tool for studying viruses and developing novel antiviral strategies, particularly when combined with the valuable platform provided by HepG2 cells. The objectives of the project were to achieve optimal particle size, stability and nucleic acid loading capacity for cross-linked Cts-NPs to ensure efficient delivery. This optimization process involved investigating how these parameters influence the ability of NPs to encapsulate and protect nucleic acids. We evaluated the ability of Cts-NPs to complex with nucleic acids, their cellular absorption, and transfection efficiency in various cell lines. This comprehensive in vitro evaluation provided insights into the potential of Cts-NPs for intracellular nucleic acid delivery. Additionally, in vivo studies were conducted to assess the biodistribution, targeting potential, and therapeutic efficacy of Cts-NP-based nucleic acid delivery systems. These experiments elucidated the actual behavior of Cts-NPs within an organism and their effectiveness in delivering nucleic acids to target sites. By addressing these objectives, this research aimed to significantly contribute to the development of a safe, efficient, and versatile Cts-NP platform for nucleic acid delivery. This platform has the potential to advance gene therapy and other therapeutic approaches utilizing nucleic acids.

2. Material and Methods

2.1. Chemicals and Materials

The following materials were used to prepare cross-linked Cts-NPs. Cts with medium molecular weight of 190,000–310,000 Da, deacetylation degree of 75–85 %, acetic acid glacial (AcOH) (98 %), hydrochloric acid (HCl, 98%) and sodium hydroxide (NaOH, 99%) all were analytical grade and obtained from Sigma-Aldrich, USA. The chemicals were used without further purification.

2.2. Cell Lines and Culture Reagents

The cell lines used in this study were obtained from the American Type Culture Collection (ATCC). Cells were cultured in Dulbecco's Modified Eagle Medium (DMEM, Gibco) supplemented with 10% fetal calf serum (FCS, Gibco), 2 mM L-glutamine (Gibco), and 1% penicillin-streptomycin (Pen-Strep, Gibco).

2.3. Medium Preparation

To prepare the complete growth medium, we supplemented DMEM with 10% fetal calf serum (FCS), 2 mM L-glutamine, and 1% penicillin-streptomycin solution under sterile conditions in a laminar flow hood. The medium was then filtered through a 0.22 μm filter to ensure sterility and stored at 4°C for up to two weeks.

2.4. Preparation of Cross-linked Cts-NPs

A solution of 100 mL double-distilled water (DDW) was mixed with 250 µL of acetic acid (AcOH) until the pH reached approximately 4.2. To prepare the Cts solution, 0.2331 g of Cts powder was added to 70 mL of the acidic solution and stirred for 10 minutes until a clear solution was obtained (S0). This solution was then used to prepare seven Cts-NPs samples, cross-linked with TPP at 0.05, 0.1, 0.11, 0.15, 0.2, 1.0, and 2.0 molar ratios (S1 to S7). During the continuation of the reaction, a homogenizer was used, and 10 mL of the TPP solution with the specified molar ratio was gradually added to 10 mL of the Cts solution, which was homogenized for 10 minutes at 15,000 rpm.

2.5. Loading of Cross-linked Cts-NPs with DNA

The preparation of cross-linked chitosan nanoparticles (Cts-NPs) loaded with DNA involved the use of solutions at two different molar ratios of TPP to Cts (0.11 and 0.15 w/w). Distilled water (dH2O) was used as the solvent in all preparations. For the DNA-NP mixture preparation, twenty microtubes were allocated, with ten dedicated to NP mixtures and ten to DNA mixtures. For the NP mixtures, solutions with a molar ratio of TPP to Cts of 0.11 were prepared in three sets with NP to DNA weight ratios of 1:1 (0.00333 µg DNA/µl), 1:2, and 1:5. Aliquots of 50 µl and 100 µl of the 0.11 NP solution were used for each set, and the microtubes were labeled to indicate the NP to DNA weight ratios and volume. Similarly, for the molar ratio of TPP to Cts of 0.15, mixtures with NP to DNA weight ratios of 1:1, 1:2, and 1:5 was prepared, using 50 µl and 100 µl aliquots of the NP solution (excluding 50 µl solutions). Each tube was labeled to indicate the specific DNA:NP ratio, volume, and type of NP solution used. Microtubes containing NP mixtures, except for the 50 µl solutions, were centrifuged at 10,000 rpm for six minutes at 45°C. After centrifugation, the supernatant was removed, and the nanoparticles were resuspended in approximately 50 µl dH2O. For the DNA mixtures, three microtubes were prepared with 3 µl DNA and 50 µl opti-medium (DMEM). The remaining tubes were prepared with 3 µl DNA, 22 µl dH2O, and 25 µl Na2SO4. All microtubes containing DNA or NP mixtures were incubated at 45°C for 15 minutes at 700 rpm in a shaking incubator. Following incubation, the DNA mixtures were combined with their corresponding NP mixtures and further incubated for one hour at 37°C at 700 rpm. During transfection, approximately 100 µl of each DNA-NP mixture was added to designated wells on two cell plates, with each well labeled to identify the DNA:NP ratio and cell line. This process was repeated twice for both cell plates to ensure adequate replicates. Control mixtures were also prepared: one with 50 µl opti-medium and 3 µl DNA to serve as a naked DNA control, and another with 50 µl opti-medium and 2 µl lipofectamine. These control mixtures were incubated at room temperature for five minutes before combining and further incubating for 15 minutes, after which the lipofectamine-DNA complex was added to the cells. Established cell culture protocols were followed for HEK293 and HepG2 cell lines. Cells were maintained in T75 flasks at 37°C in a humidified atmosphere with 5% CO_2. The culture medium was changed every 2-3 days to provide fresh nutrients and remove metabolic waste. Cells were passaged at approximately 80% confluency using a 0.05% trypsin-EDTA solution. Trypsinization was performed by rinsing the cells with PBS to remove serum, followed by the addition of trypsin-EDTA. Cells were incubated at 37°C until detachment, neutralized with an equal volume of complete medium, and centrifuged at 300 x g for five minutes. The supernatant was discarded, and the cell pellet was resuspended in fresh medium, counted using a hemocytometer, and reseeded at a density of 1×10^4 cells/cm² for further experiments. For cryopreservation, cells were resuspended in a freezing medium consisting of 90% FCS and 10% DMSO at a concentration of 1×10^6 cells/mL, aliquoted into cryovials, and gradually frozen at -1°C per minute using an isopropanol freezing container. Cryovials

were stored in liquid nitrogen. To thaw cells, cryovials were quickly warmed in a 37°C water bath and transferred to a T75 flask with pre-warmed complete medium. Cells were allowed to recover overnight before passaging or use in experiments. Quality control involved regular monitoring of cell morphology using a phase-contrast microscope, monthly mycoplasma contamination tests, and viability assessments using trypan blue exclusion assay. Only mycoplasma-free cells with viability greater than 95% were used. Cell seeding densities were calculated after incubation and counting with a hemocytometer, with HEK293 cells prepared at 2.16 x 10^6 cells/ml and HepG2 cells at 2.5 x 10^6 cells/ml, using a seeding volume of 50 µl per well.

2.6. Physicochemical Characterization

The DNA loaded with Cts-NPs were analyzed by ultraviolet-visible (UV–vis) spectrophotometry (Cary 60, Agilent) in the range of 200–700 cm^{-1}. For Fourier transform infrared (FTIR) spectroscopy, the sample was analyzed using ATR method and the spectra of the samples were analyzed under a transmittance mode from 4000 to 400 cm^{-1} with a 4 cm^{-1} resolution and an accumulation of 128 scans. Dynamic light scattering (DLS) and zeta potential measurements were performed on a Zeta Sizer Nanoseareis (SZ Malvern instrument) all samples were analyzed at angle of 172° and a temperature of 25°C. The morphology of the NPs was examined using Transmission Electron Microscopy (TEM). A drop of aqueous Cts-NPs suspension was deposited on a carbon-coated electron microscope grid and then allowed to dry in oven under vacuum for 24 hours to ensure the complete dryness of the sample. The grids were observed with a Hitachi HF2000 TEM operated at an accelerating voltage of 80 kV.

2.7. Preparation of Reagent Mixtures

Lipofectamine 3000, Transfex, and Fugene as the transfection agents were selected as reagents. DNA is used as the control for HEPG2 and HEK293 cells. A 24-well plate was prepared, divided into two sections: one for HEPG2 cells and one for HEK293 cells. In each section, we designated two wells for Fugene, two wells for Transfex, and two wells for Lipofectamine 3000. For each Fugene well, we mixed 2 µl of DNA, 2 µl of Fugene, and 96 µl of medium. For each Transfex well, we combined 2 µl of DNA, 2 µl of Transfex, and 96 µl of medium. For the Lipofectamine 3000 wells, we used two microtubes. In the microtubes, we added 2 µl of DNA and 2 µl of Lipofectamine 3000.

2.8. Cell Loading Analysis

GFP fluorescence was analyzed using an epifluorescence microscope equipped with a GFP filter set (excitation/emission: 488 nm/507 nm). Images were captured using a digital camera attached to the microscope and processed with imaging software. Post-transfection, the culture medium was removed, and cells were washed twice with phosphate-buffered saline (PBS). Fresh complete medium was added before imaging. Cells expressing GFP were visualized and images were acquired at multiple fields of view to ensure representative sampling of transfection efficiency. For the Acquisition of DNA Loading in the selected cell lines, The NanoDrop 2000/2000c Spectrophotometer (Thermo Fisher Scientific) was initialized and calibrated using a blank sample (nuclease-free water) according to the manufacturer's instructions. The NanoDrop software was launched, and the appropriate nucleic acid measurement module (DNA) was selected. The software settings were configured to measure absorbance at 260 nm (A260) for DNA quantification and at 280 nm (A280) for purity assessment.

2.9. Cytotoxicity Assay for DNA Loading Using CellTiter-Blue (CTB) Reagent

HepG2 and HEK293 cells were cultured in Dulbecco's Modified Eagle Medium (DMEM) supplemented with 10% fetal bovine serum (FBS), 1% penicillin-streptomycin, and 2 mM L-glutamine. Cells were maintained in a humidified atmosphere of 95% air and 5% CO_2 at 37°C. CellTiter-Blue (CTB) Cell Viability Assay (Promega) was used to assess cytotoxicity. The CTB reagent was prepared according to the manufacturer's instructions. After the transfection period, 20 µL of CellTiter-Blue reagent was added to each well containing 100 µL of medium. The plate was gently shaken to ensure thorough mixing and then incubated for 1-4 hours at 37°C in a humidified, 5% CO_2 atmosphere. Fluorescence was measured using a plate reader with excitation/emission wavelengths of 560 nm/590 nm. The fluorescence intensity directly correlates with the number of viable cells, allowing assessment of cytotoxicity induced by the transfection process. The fluorescence readings from the CTB assay were recorded. The data were normalized to the untreated control wells to calculate the percentage of cell viability.

3. Results and Discussion

3.1. Zeta Potential, Particle size and Polydispersity Index Studies

The initial zeta potential (ζ-potential) of the Cts solution (S0) was positive, measured at +38.85 mV. As the molar ratio of TPP to Cts increased to produce cross-linked Cts-NPs, ζ-potential values gradually decrease, starting from +42.94 mV (S1) and reaching to -0.12 mV (S7). This trend shows that the gradual decrease in the surface charge of Cts-NPs occurred with the increase in the TPP ratio. Among the samples, the results for S1 to S3 indicated that, despite a slight increase in ζ-potential in S1 followed by a decrease in S2 and S3, but there was no significant difference in their ζ-potential compared to Cts solution. The ζ-potential decreases from S3 to S7. Notably, samples S1 and S2, despite having high ζ-potential, were not selected as optimum due to their low efficiency. Instead, S3 and S4 were chosen for their higher efficiency and ability to be collected effectively. Therefore, S3 and S4 with ζ-potential of +28.76 and +13.11mV can be selected as optimal samples. Since the positive charge of cross-linked Cts-NPs was crucial for and binding to nucleic acids (DNA, RNA, etc..), it makes these two samples the most effective choice. Overall, the analysis showed a significant decrease in ζ-potential and its standard deviation in samples S1 to S7, with values decreasing from +42.94 ± 1.37 to 0.12 ± 0.04 mV, indicating a decrease in the potential in the binding of NPs with It will be nucleic (Table 1). Meanwhile, the cross-linked Cts-NPs could be produced at molar ratios exceeding TPP and with the increased of the production efficiency, the polydispersity index (PDI) of the Cts-NPs gradually decreases from S1 to S7 (Table 2).

Table 1
Optimal ζ-potential values for Cts and cross-linked Cts-NPs

Samples	ζ-potential (mV)				
	R1	R2	R3	Mean	± SD
S0	+41.33	+38.85	+36.37	+ 38.85	± 2.02
S1 (0.05)	+41.05	+43.52	+44.24	+ 42.94	± 1.37
S2 (0.1)	+38.68	+39.32	+38.68	+ 38.89	± 0.30
S3 (0.11)	+27.76	+29.87	+28.66	+ 28.76	± 0.86
S4 (0.15)	+12.77	+12.89	+13.68	+ 13.11	± 0.40
S5 (0.2)	+9.57	+9.82	+9.41	+ 9.60	± 0.17
S6 (1.0)	+1.18	+1.07	+1.28	+ 1.17	± 0.08
S7 (2.0)	−0.17	−0.068	−0.13	− 0.12	± 0.04

* SD: Standard deviation; R: Replicate, S1 to S7: Cross-linked Cts-NPs (0.05, 0.1, 0.11, 0.15, 0.2, 1.0 and 2.0) respectively.

Table 2
Optimal polydispersity index (PDI) values for cross-linked Cts-NPs

Samples	PDI				
	R1	R2	R3	Mean	± SD
S0	-	-	-	-	-
S1 (0.05)	0.40	0.42	0.47	0.43	± 0.03
S2 (0.1)	0.42	0.45	0.48	0.45	± 0.02
S3 (0.11)	0.42	0.45	0.47	0.44	± 0.02
S4 (0.15)	0.43	0.46	0.48	0.46	± 0.02
S5 (0.2)	0.43	0.48	0.51	0.47	± 0.03
S6 (1.0)	0.51	0.56	0.60	0.55	± 0.03
S7 (2.0)	0.64	0.68	0.72	0.70	± 0.04

* SD: Standard deviation; R: Replicate, S1 to S7: Cross-linked Cts-NPs (0.05, 0.1, 0.11, 0.15, 0.2, 1.0 and 2.0) respectively.

Table 3 shows that the hydrodynamic size of Cts-NPs gradually increases from S1 to S7. These values indicate a trend where the NPs size increase correlates with a decrease in both surface charge and PDI. This reduction in surface charge and PDI implies that the surface adsorption capacity of the NPs to bind with nucleic acids diminishes as the NP size grows. The surface adsorption capacity is crucial because it determines how effectively the NPs can encapsulate and protect nucleic acids for delivery. When the NPs are too large, their reduced surface charge and lower PDI mean they have less surface area and fewer active sites available for binding nucleic acids. This makes them less efficient in nucleic acid delivery. Therefore, the results suggest that the particle sizes in the S3 and S4 samples are optimal. These samples likely have a balanced size that maximizes surface charge and maintains an adequate PDI, enhancing their ability to adsorb nucleic acids effectively. This balance is crucial for ensuring efficient delivery and protection of nucleic acids, which is a key objective of the project.

Table 3
Optimal hydrodynamic size values for cross-linked Cts-NPs

Samples	Average Particle Size				
	R1	R2	R3	Mean	± SD
S0	-	-	-	-	-
S1 (0.05)	19.53	18.57	16.76	18.28	± 1.14
S2 (0.1)	20.64	19.58	22.34	20.85	± 1.13
S3 (0.11)	21.32	23.54	22.84	22.56	± 0.93
S4 (0.15)	23.56	24.38	23.27	23.73	± 0.47
S5 (0.2)	26.33	25.98	27.58	26.63	± 0.68
S6 (1.0)	30.28	33.24	31.38	31.63	± 1.22
S7 (2.0)	33.17	35.68	32.13	33.66	± 1.50

3.2. UV-visible Spectroscopy

UV-visible spectroscopy results indicate that Cts dissolved in an acetic acid medium with a pH of 4.2 shows no absorbance peak in the wavelength range of 200-700 nm, suggesting that Cts itself does not absorb light in this region. In contrast, the DNA solution exhibits a distinct absorbance peak at 260 nm, which is characteristic of nucleic acids and is used to identify and quantify DNA. When cross-linked Cts-NPs (S3) was analyzed, they also show no peak in the region, indicating that they did not absorb at this wavelength either. However, when these Cts-NPs for S3 sample was loaded with DNA, a small peak appears around 260 nm. This peak suggests that DNA is present on the surface of the NPs. The appearance of this peak in the DNA-loaded Cts-NPs confirms that an electrostatic bond has formed between the positively charged surface of the Cts-NPs and the negatively charged DNA (Figure 4).

This interaction is due to the attraction between the opposite charges, which facilitates the binding of DNA to the NPs. The presence of this peak in the loaded NPs demonstrates that the DNA has been successfully loaded onto the Cts-NPs to a certain degree. This specific binding is crucial for the intended application, as it confirms that the NPs can effectively carry and potentially deliver nucleic acids. The degree of nucleic acid loading is essential for the efficiency of delivery systems in therapeutic applications, ensuring that an adequate amount of genetic material is transported to target cells. In summary, the UV-visible spectroscopy results provide clear evidence of the successful binding of DNA to Cts-NPs, validating their potential use as carriers in nucleic acid delivery systems.

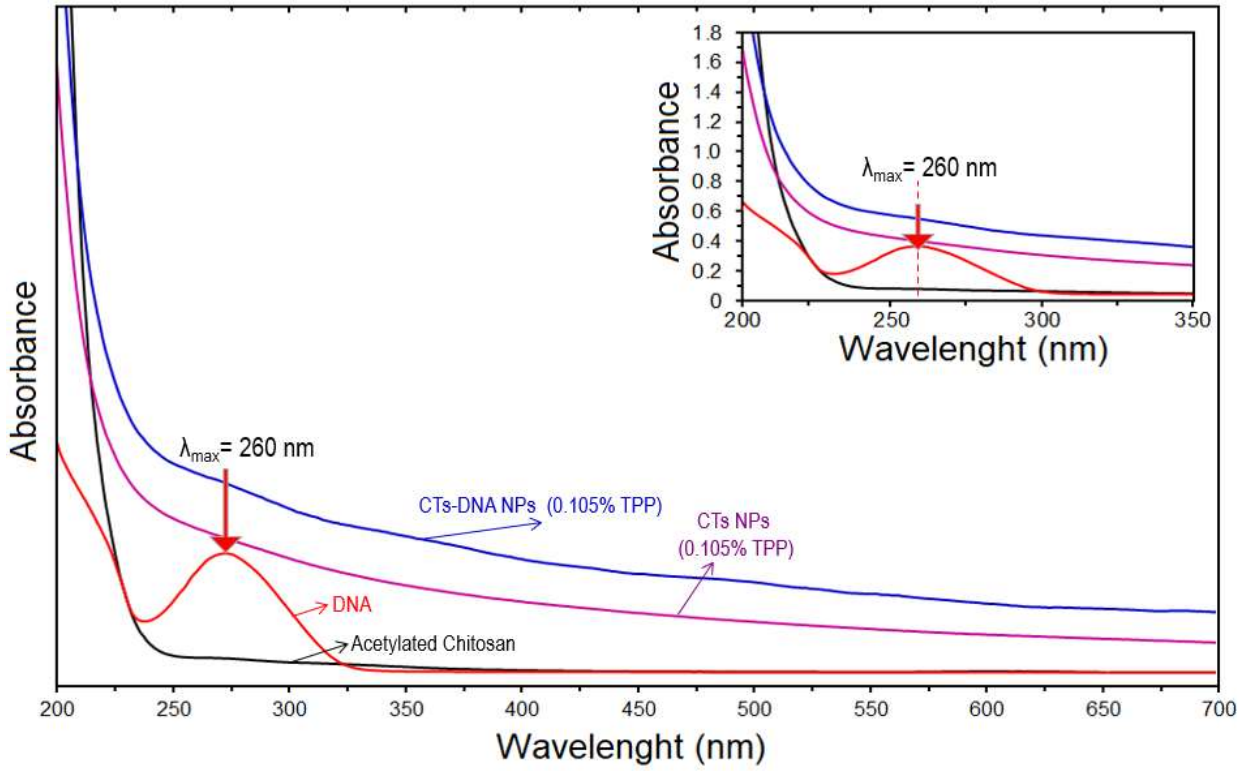

Fig. 4. UV-visible spectroscopy results for acetylated Cts, DNA, Cts-NPs and DNA loaded Cts-NPs (S3), respectively

3.3. Fourier Transform Infrared Spectroscopy

The FTIR spectroscopy provided valuable insights into the structural characteristics and interactions within the Cts-NPs. The similarities in the spectra of Cts, cross-linked Cts-NPs, and DNA-loaded NPs indicated that the fundamental chemical structure of Cts remained intact during the nanoparticle formation and DNA loading processes. The peak observed in the wavelength range of 1225-1220 cm^{-1}, attributed to the antisymmetric DNA-phosphate stretching, highlighted the presence of DNA in the NPs. This particular peak indicated the successful incorporation of DNA into the Cts-NPs, facilitated by van der Waals interactions. The appearance of this peak was crucial because it confirmed that the DNA was not merely adsorbed on the surface but was effectively interacting with the NPs. Additionally, the peak appearing at 970–965 cm^{-1} indicated that an electrostatic connection had been established, specifically the formation of a P-O-P bond between DNA and Cts. This bond formation was a key aspect of the interaction mechanism, indicating that the phosphate groups of DNA interacted electrostatically with the amine groups of Cts. This electrostatic interaction was essential for the stability of the DNA-loaded NPs, ensuring that the DNA was securely bound within the NPs matrix. Two relatively long peaks in the wavelength range of 1500–1700 cm^{-1} were very important as they confirmed cross-linking within the NPs. Cross-linking is a critical process that increases the structural integrity and stability of NPs. The existence of these peaks showed that a regular structure had formed inside the NPs, which is essential for their performance in biological applications. This regular and stable structure ensured that the NPs could effectively protect DNA from degradation and facilitate its controlled release (Figure 5).

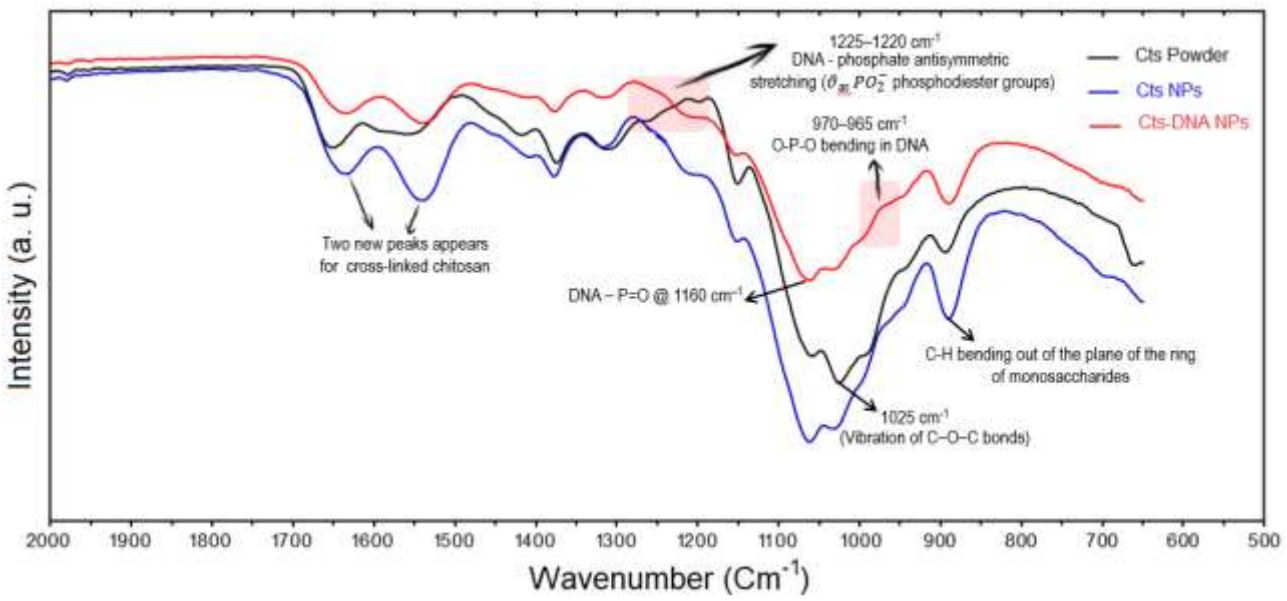

Fig. 5. FTIR results for acetylated Cts powder, Cts-NPs and DNA loaded Cts-NPs (S3), respectively

3.4. Transmission Electron Microscope Study

The transmission electron microscope (TEM) analysis of sample S3, with its accompanying histogram, provides detailed insights into the size and morphology of the cross-linked Cts-NPs. The measured average size of the NPs is 8.79±2.23 nm, based on a count of approximately 119 particles. This precise size distribution is crucial for ensuring consistency and reliability in various applications, particularly in the field of drug delivery and biomedical research. The TEM images (Figure 6) reveal several key characteristics of the Cts-NPs. Firstly, the NPs are predominantly spherical in shape, which is often associated with improved cellular uptake and less cytotoxicity compared to irregularly shaped particles. The uniform distribution observed in the TEM images indicates a well-controlled synthesis process, which is essential for reproducibility and scalability in practical applications. The abundance of particles further suggests that the synthesis method is efficient, producing a high yield of NPs. The choice of S2 as the optimum sample is further supported by additional characterization techniques. The ζ-potential measurement provides information about the surface charge of the NPs, which is a critical factor in determining their stability in suspension and their interaction with biological membranes. A suitable ζ-potential ensures that the NPs remain dispersed and do not aggregate, which is important for maintaining their functionality. The PDI is another important parameter that reflects the uniformity of the particle size distribution.

A low PDI indicates a narrow size distribution, which is desirable for uniform behavior in biological systems. Consistent particle size and distribution contribute to predictable pharmacokinetics and biodistribution, enhancing the efficacy of NP-based delivery systems. The hydrodynamic size, determined through DLS, provides additional confirmation of the NP size in a hydrated state, which is how they will exist in biological environments. The hydrodynamic size is typically larger than the TEM-measured size due to the hydration layer around the NPs. The agreement between the hydrodynamic size and the TEM measurements further validates the integrity of the NP characterization. These combined results demonstrate that sample S2 possesses the optimal characteristics for nucleic acid loading. The appropriate size, shape, surface charge, and uniform distribution of the Cts-NPs make them suitable candidates for delivering nucleic acids, potentially enhancing their stability, cellular uptake, and therapeutic efficacy. Consequently, S2 represents a

promising formulation for further development in nucleic acid-based therapies and other biomedical applications.

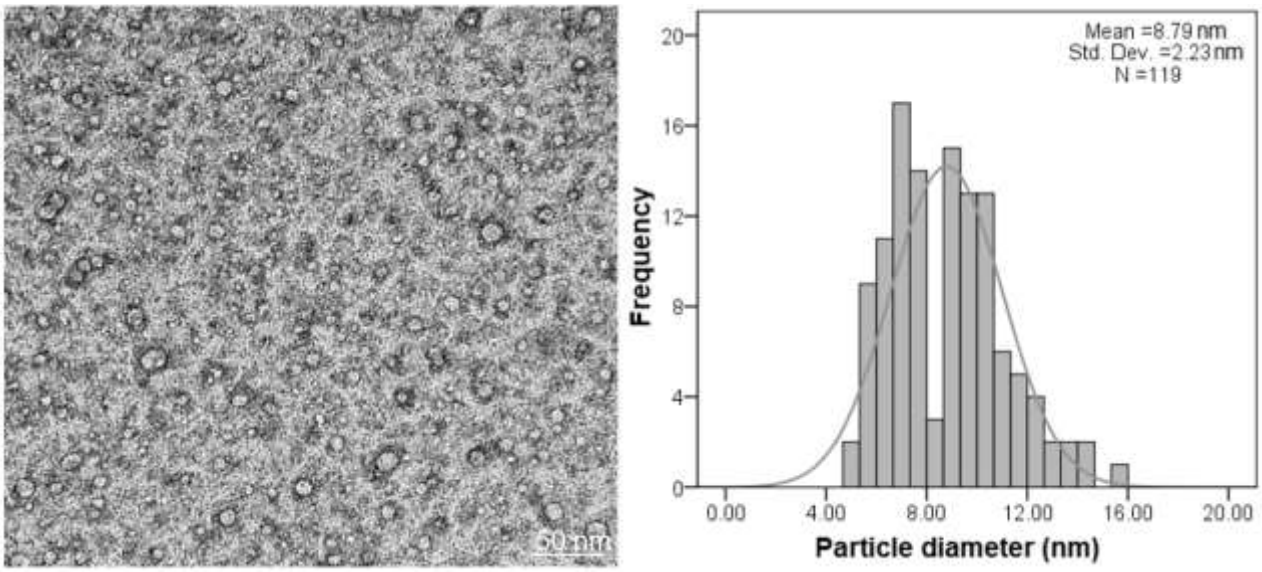

Fig. 6. The TEM and histogram results for the Cts-NPs sample (S3) confirm their spherical shape and size range of approximately 6.56–11.02 nm

3.5. Nucleic Acid Concentration and Purity Analysis Using UV-Nanodroplets

The concentration and purity of the extracted nucleic acids were determined using a NanoDrop spectrophotometer. The absorbance spectra of the samples were recorded across the UV range from 200 nm to 800 nm. The absorbance spectra for DNA samples displayed a distinct peak at 260 nm, indicative of nucleic acid presence. The concentration of DNA was calculated using the absorbance at 260 nm, applying the Beer-Lambert law with an extinction coefficient of 50 ng/μL for double-stranded DNA. The average concentration of DNA across the samples was determined to be 100 ng/μL. To assess the purity of the DNA samples, the A260/A280 ratio was calculated. The A260/A280 ratio for all DNA samples ranged from 1.8 to 2.0, indicating high purity with minimal protein contamination. Additionally, the A260/A230 ratio, which helps detect other contaminants such as phenol or carbohydrates, was found to be within the acceptable range of 2.0 to 2.2 for most samples, suggesting the samples were free from significant impurities.

By reporting these results and interpretations, the integrity and quality of the samples are validated, providing a solid foundation for subsequent experimental procedures. In UV NanoDrop spectrophotometer, the X-axis represents the wavelength of light in nanometers. The range often includes wavelengths from 200 nm to 800 nm, which covers the UV and visible spectrum. The Y-axis represents the absorbance (also known as optical density, OD) of the sample at each wavelength. Absorbance is a measure of how much light is absorbed by the sample at a particular wavelength. The UV nanodrop spectrometry was performed for each sample and they were compared (Figure 7). The sample with the 0.11 molar ratio of TPP to Cts with 1:1 NP to DNA weight ratio shows the highest peak indicating highest absorbance and purity compared to the other samples supporting the previous findings.

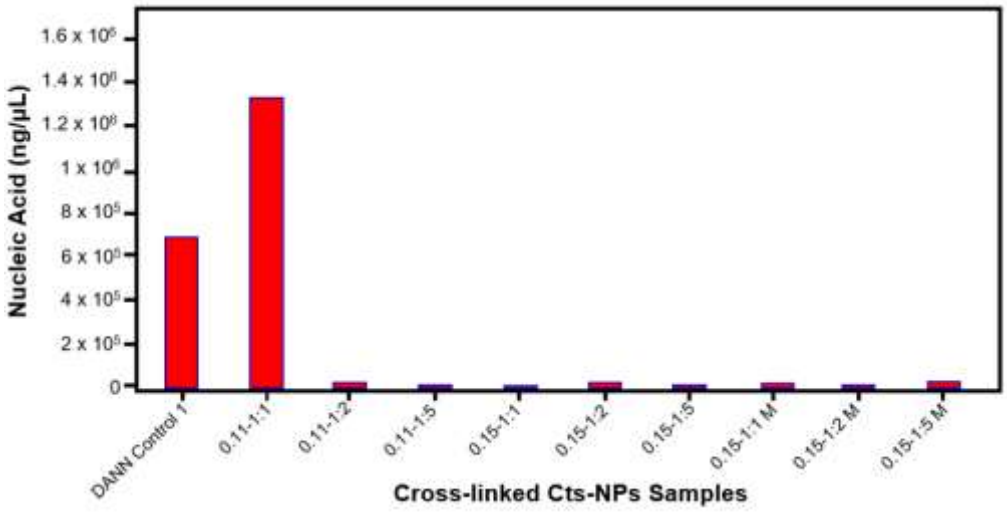

Fig. 7. The result of UV-NanoDrop showing the transfection and absorption of the Cts-NPs have occurred positively

3.6. Transfection Efficiency: Lipofectamine 2000 vs. Cts-NPs

The expression and localization of GFP in transfected cells were analyzed using fluorescent microscopy. Cells were observed and imaged under a microscope equipped with appropriate filters for GFP detection, using an excitation wavelength of 488 nm and an emission wavelength of 509 nm. Transfection using the reagent Lipofectamine 2000 resulted in bright green fluorescence in transfected cells, indicating successful expression of GFP. The fluorescence was primarily localized in the cytoplasm and, in some cases, the nucleus, depending on the construct used for transfection. In contrast, cells transfected with Cts-NPs showed minimal or no fluorescence, indicating poor transfection efficiency with those methods. Non-transfected control cells did not show any fluorescence, confirming the specificity of GFP expression in cells treated with Lipofectamine 2000.

Quantitative analysis revealed that approximately 70% of the cells transfected with Lipofectamine 2000 expressed GFP, as determined by counting the number of fluorescent cells relative to the total number of cells observed in multiple fields of view. This high transfection efficiency indicates the effectiveness of Lipofectamine 3000. Cells loaded with Cts-DNA nanoparticles resulted in less than 10% GFP-positive cells, highlighting the superior performance of Lipofectamine 2000 (Figure 8).

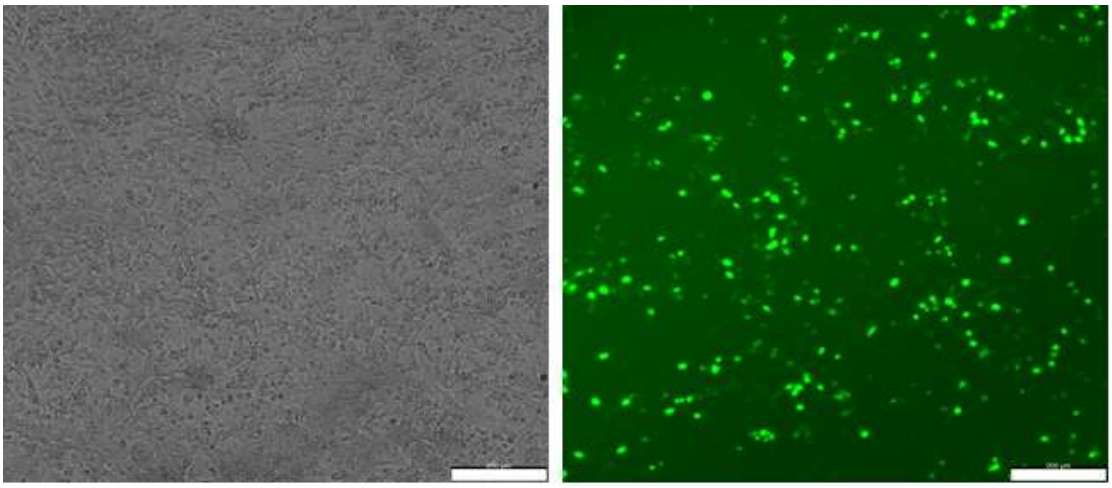

Fig. 8. The result of the fluorescent imagery of Lipofectamine 2000 with HepG2 cell mixture after loading with S3 showing positive results with this reagent

3.7. Evaluating Transfection Reagents in HepG2 and HEK293 Cells

The fluorescence intensity of GFP in cells transfected with Lipofectamine 2000 was significantly higher compared to those transfected with other reagents. The mean fluorescence intensity per cell, calculated using image analysis software, was 1400 arbitrary units (AU) for Lipofectamine 2000, whereas cells transfected with Cts-DNA nanoparticles showed mean intensities below 300 AU. The results from the GFP fluorescent microscopy analysis demonstrate that Lipofectamine 3000 is highly effective for transfection, leading to robust GFP expression in a majority of cells. The high transfection efficiency and fluorescence intensity observed with Lipofectamine 2000 underscore its effectiveness compared to Cells loaded with Cts-DNA nanoparticles, which showed minimal GFP expression. Several factors could explain why the transfection of HepG2 and HEK293 cells with Cts-DNA nanoparticles did not result in detectable fluorescent signals. Transfection efficiency can vary significantly depending on the cell type. HepG2 cells, derived from human liver carcinoma, have shown moderate transfection efficiency with various methods, including lipofection and polycation-based systems like Cts-NPs. However, their uptake rate can be influenced by factors such as cell density, the presence of serum in the culture medium, and the specific transfection reagent used (Figure 8). The endocytosis rate and intracellular trafficking mechanisms in HepG2 cells might lead to variable results, sometimes resulting in lower transfection efficiency compared to other cell lines such as HeLa or HEK293 [40, 41]. HEK293 cells, derived from human embryonic kidney cells, are well-known for their high transfection efficiency with many transfection methods, including lipofection and electroporation. These cells are often used as a standard for comparing transfection efficiencies due to their robustness and consistent performance [42]. Despite their generally high transfection efficiency, there can be instances where certain delivery systems, such as Cts-NPs, may not perform as well. This variability can be due to differences in nanoparticle uptake mechanisms and intracellular processing [43]. Cytotoxicity induced by Cts-NPs can also impair cell health and viability, thus reducing overall transfection efficiency. If the cells are adversely affected by the nanoparticles, they may not support the expression of the transfected gene. Furthermore, variations in experimental conditions, such as the ratio of Cts to DNA, incubation time, and the presence of serum in the culture medium, can significantly impact transfection outcomes. Optimization of these parameters is crucial for achieving detectable gene expression [44].

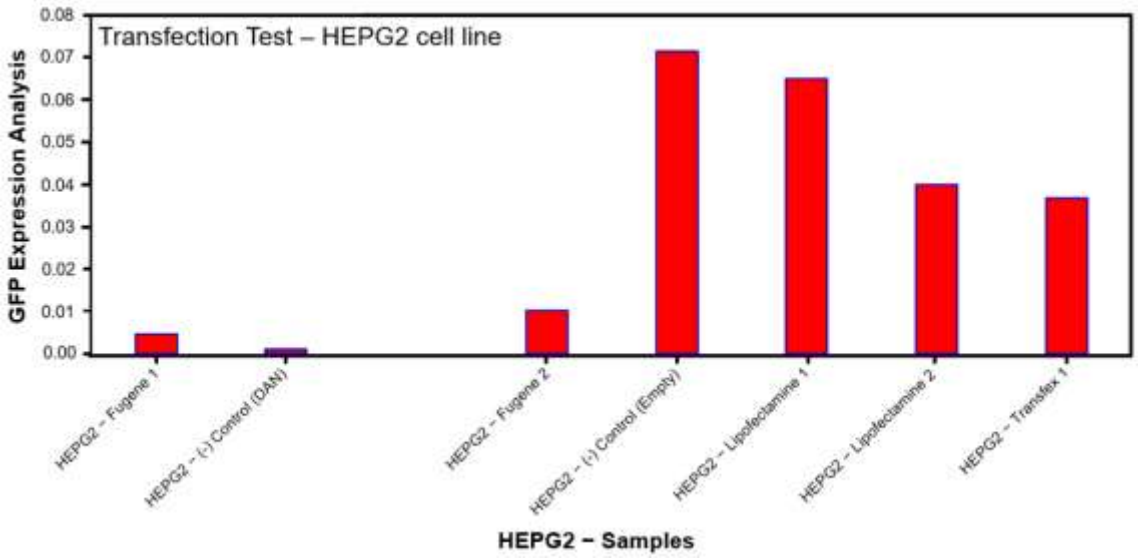

Fig. 9. Transfection efficiency and GFP expression analysis indicating lipofectamine transfection efficiency

The effectiveness of various transfection reagents in delivering plasmids into HepG2 and HEK293 cell lines was assessed using a transient transfection test machine, which provided quantitative analysis and graphical results of cell growth and transfection efficiency. The reagents tested included Lipofectamine 3000, Transfex, and Fugene. Lipofectamine 3000 demonstrated the highest transfection efficiency in both HepG2 and HEK293 cell lines. Graphical analysis from the transient transfection test machine showed a significant increase in cell growth and transfection rates. In both cell lines, over 70% of the cells were successfully transfected, as indicated by the high transfection efficiency graphs. Additionally, the cell growth graphs indicated robust cell proliferation post-transfection, with HEK293 cells showing slightly higher growth rates compared to HepG2 cells. This suggests that Lipofectamine 3000 is highly effective in promoting both transfection and cell growth in these cell lines (Figure 9).

Transfex facilitated successful transient transfection in both HepG2 and HEK293 cell lines, but to a lesser extent than Lipofectamine 3000. It is shown that approximately 40% of the cells were transfected with Transfex. HEK293 cells exhibited higher transfection rates and cell growth compared to HepG2 cells, as evidenced by the respective graphs. The cell growth graphs indicated moderate cell proliferation, suggesting that Transfex is a viable but less effective alternative for transfection in these cell lines. Fugene was the least effective transfection reagent in this study. The transfection efficiency graphs showed that less than 10% of the cells were transfected in both HepG2 and HEK293 cell lines. Correspondingly, the cell growth graphs indicated minimal cell proliferation post-transfection, suggesting that Fugene did not facilitate efficient plasmid delivery or promote cell growth in either cell line.

Non-transfected control cells, which did not receive any transfection reagent, served as a baseline for the analysis. The control graphs showed no significant increase in transfection efficiency and maintained normal cell growth rates, confirming that the observed effects in transfected cells were due to the successful delivery and expression of the plasmid. The results from the transient transfection test machine indicate that Lipofectamine 3000 is highly effective for transient plasmid delivery in both HepG2 and HEK293 cell lines, demonstrating superior transfection efficiency and promoting robust cell growth. The graphical data highlight that HEK293 cells generally respond better to transfection, showing higher growth and transfection rates compared to HepG2 cells. Transfex provided moderate transfection efficiency and cell growth, making it a viable alternative but less effective than Lipofectamine 3000. Fugene showed the least effectiveness in both cell lines, with minimal transfection and cell proliferation. These findings emphasize the reliability and effectiveness of Lipofectamine 3000 for high-efficiency transient transfection and underscore its utility in various cells.

3.8. Cytotoxicity and Efficiency of Transfection Reagents in Cell Lines

The cytotoxicity and transfection efficiency of three transfection reagents —Transfex, Fugene, and Lipofectamine 3000—were evaluated in three cell lines: HepG2, HEK293, and Huh7. Each cell line was cultured in a 24-well plate, with two wells assigned to each transfection reagent. The GFP expression was used to assess transfection efficiency, while the CellTiter-Blue (CTB) assay was employed to measure cell viability and cytotoxicity. The GFP expression graphs indicated that Transfex was the most effective reagent for transfecting HEK293 and Huh7 cells, resulting in the highest GFP fluorescence intensity. In contrast, Lipofectamine 3000 demonstrated the highest transfection efficiency in HepG2 cells. Fugene showed the lowest GFP expression intensity across all three cell lines, indicating it was the least effective transfection reagent. The CTB assay results provided insights into the cytotoxic effects of the transfection reagents.

While Transfex was effective in transfecting HEK293 and Huh7 cells, it exhibited significant cytotoxicity in HEK293 cells. The CTB graphs showed a clear reduction in biological metabolism in HEK293 cells treated with Transfex, indicating lower cell viability. In Huh7 cells, the cytotoxicity of Transfex was less pronounced, with moderate reductions in cell viability observed. In HepG2 cells, Transfex showed minimal cytotoxicity. This reagent was highly effective in transfecting HepG2 cells but also exhibited high cytotoxicity in these cells. The CTB graphs for HepG2 cells transfected with Lipofectamine 3000 showed significant reductions in cell viability, indicating a high level of toxicity. In HEK293 and Huh7 cells, Lipofectamine 3000 showed lower levels of cytotoxicity compared to Transfex, with moderate to minimal reductions in cell viability observed. Fugene demonstrated the lowest transfection intensity, as evidenced by the GFP expression graphs, and correspondingly showed low cytotoxicity effects in all three cell lines. The CTB graphs indicated minimal reductions in cell viability across HepG2, HEK293, and Huh7 cells, suggesting that Fugene was the least toxic transfection reagent (Figure 10).

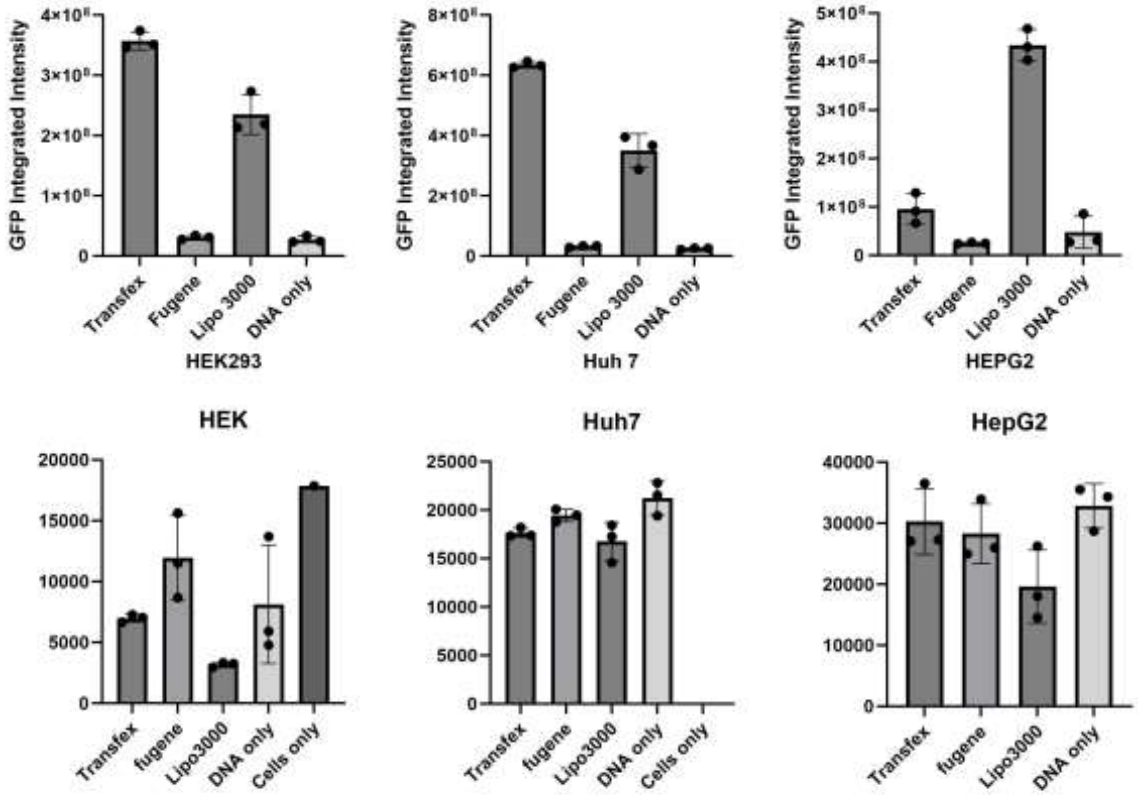

Fig. 10. CellTiter-Blue® Cell Viability Assay (CTB) and transfection efficiency analysis

The results from the CellTiter-Blue® Cell Viability Assay (CTB) and GFP expression analyses highlight the differential effects of transfection reagents on cell viability and transfection efficiency in HepG2, HEK293, and Huh7 cell lines. Transfex emerged as the most effective reagent for transfecting HEK293 and Huh7 cells, but its high cytotoxicity in HEK293 cells limits its utility in this cell line. Lipofectamine 3000 was most effective for transfecting HepG2 cells; however, its high cytotoxicity in these cells is a significant drawback. Fugene, while showing the lowest transfection efficiency, also exhibited the least cytotoxicity, making it a safer option when minimal cell damage is a priority (Figure 10). These findings emphasize the importance of balancing transfection efficiency with cytotoxicity when selecting a transfection reagent. For HEK293 cells, despite Transfex's high

transfection efficiency, its cytotoxicity suggests that alternative methods or reagents may be necessary. For HepG2 cells, the high efficiency of Lipofectamine 3000 must be weighed against its cytotoxic effects. The low cytotoxicity of Fugene, although coupled with low transfection efficiency, presents it as a potentially useful reagent for applications where cell viability is critical. These results underscore the necessity of comprehensive evaluations combining both transfection efficiency and cytotoxicity to guide the selection of optimal transfection reagents for different cell lines and experimental objectives.

4. Conclusions

In conclusion, this study successfully optimized chitosan nanoparticles (Cts-NPs) for nucleic acid delivery by varying the molar ratio of tripolyphosphate (TPP) to Cts, focusing on their ζ-potential, size, polydispersity index (PDI), and binding efficiency. The ζ-potential of the Cts solution initially at +38.85 mV, decreased from +42.94 mV (S1) to -0.12 mV (S7) as the TPP ratio increased. Among these, samples S3 and S4, with ζ-potentials of +28.76 mV and +13.11 mV respectively, were identified as optimal due to their superior efficiency and ability to effectively bind nucleic acids. UV-visible spectroscopy, indicated by a peak at 260 nm, confirmed DNA binding to Cts-NPs, while FTIR analysis revealed successful incorporation of DNA into the NPs through electrostatic interactions and cross-linking, essential for stability and controlled release. TEM analysis of sample S3 showed an average NP size of 8.79 ± 2.23 nm, highlighting a spherical shape and uniform distribution, which are beneficial for cellular uptake and reduced cytotoxicity. Transfection efficiency, assessed using GFP expression in HepG2 and HEK293 cell lines, revealed that Lipofectamine 2000 achieved over 70% transfection efficiency, significantly higher than Cts-DNA NPs, which showed less than 10%. Further comparisons among transfection reagents (Lipofectamine 3000, Transfex, and Fugene) indicated that Lipofectamine 3000 exhibited the highest efficiency in both HepG2 and HEK293 cells, with over 70% transfection, albeit with high cytotoxicity in HepG2 cells. Transfex demonstrated moderate efficiency (~40%) but significant cytotoxicity in HEK293 cells, while Fugene exhibited the lowest efficiency (<10%) and minimal cytotoxicity. Overall, the optimal Cts-NPs (S3 and S4) demonstrated a balance of size, surface charge, and efficiency, making them promising candidates for nucleic acid delivery. However, Lipofectamine 3000, despite its high efficiency, poses cytotoxicity concerns. These findings underscore the necessity of balancing efficiency and cytotoxicity in selecting appropriate transfection methods for different cell lines, which is crucial for advancing gene delivery systems in therapeutic applications.

Acknowledgement

The authors extend their sincere appreciation to the Technical University of Munich for their invaluable support in facilitating the publication of this research in the Journal of Research in Nanoscience and Nanotechnology.

References

1. Paul, W., and C. P. Sharma. "Chitosan, a drug carrier for the 21* century: a review." *STP Pharma Science* 10, no. 1 (2000): 5-22.
2. Khor, Eugene, and Lee Yong Lim. "Implantable applications of chitin and chitosan." *Biomaterials* 24, no. 13 (2003): 2339-2349. https://doi.org/10.1016/S0142-9612(03)00026-7

3. Gomes, Laidson P., Cristina T. Andrade, Eduardo M. Del Aguila, Cameron Alexander, and Vânia MF Paschoalin. "Assessing the antimicrobial activity of chitosan nanoparticles by fluorescence-labeling." *International Journal of Biotechnology and Bioengineering* 12, no. 4 (2018): 112-117.
4. Ilium, Lisbeth. "Chitosan and its use as a pharmaceutical excipient." *Pharmaceutical research* 15 (1998): 1326-1331. https://doi.org/10.1023/A:1011929016601
5. Yemisci, Muge, Secil Caban, Eduardo Fernandez-Megia, Yilmaz Capan, Patrick Couvreur, and Turgay Dalkara. "Preparation and characterization of biocompatible chitosan nanoparticles for targeted brain delivery of peptides." *Neurotrophic Factors: Methods and Protocols* (2018): 443-454. https://doi.org/10.1007/978-1-4939-7571-6_36
6. Sullivan, David Joseph, Malco Cruz-Romero, Timothy Collins, Enda Cummins, Joseph P. Kerry, and Michael A. Morris. "Synthesis of monodisperse chitosan nanoparticles." *Food Hydrocolloids* 83 (2018): 355-364. https://doi.org/10.1016/j.foodhyd.2018.05.010
7. Divya, K., and M. S. Jisha. "Chitosan nanoparticles preparation and applications." *Environmental chemistry letters* 16 (2018): 101-112. https://doi.org/10.1007/s10311-017-0670-y
8. Frokjaer, Sven, and Daniel E. Otzen. "Protein drug stability: a formulation challenge." *Nature reviews drug discovery* 4, no. 4 (2005): 298-306. https://doi.org/10.1038/nrd1695
9. Janes, K. A., P. Calvo, and M. J. Alonso. "Polysaccharide colloidal particles as delivery systems for macromolecules." *Advanced drug delivery reviews* 47, no. 1 (2001): 83-97. https://doi.org/10.1016/S0169-409X(00)00123-X
10. Paul, W., and C. P. Sharma. "Chitosan, a drug carrier for the 21* century: a review." *STP Pharma Science* 10, no. 1 (2000): 5-22.
11. Calvo, Pilar, C. Remunan-Lopez, Jose Luis Vila-Jato, and M. J. Alonso. "Novel hydrophilic chitosan-polyethylene oxide nanoparticles as protein carriers." *Journal of applied polymer science* 63, no. 1 (1997): 125-132. https://doi.org/10.1002/(SICI)1097-4628(19970103)63:1<125::AID-APP13>3.0.CO;2-4
12. Janes, K. A., and M. J. Alonso. "Depolymerized chitosan nanoparticles for protein delivery: preparation and characterization." *Journal of applied polymer science* 88, no. 12 (2003): 2769-2776. https://doi.org/10.1002/app.12016
13. Gan, Quan, and Tao Wang. "Chitosan nanoparticle as protein delivery carrier—systematic examination of fabrication conditions for efficient loading and release." *Colloids and Surfaces B: Biointerfaces* 59, no. 1 (2007): 24-34. https://doi.org/10.1016/j.colsurfb.2007.04.009
14. Nasti, Alessandro, Noha M. Zaki, Piero De Leonardis, Suwipa Ungphaiboon, Proramate Sansongsak, Maria Grazia Rimoli, and Nicola Tirelli. "Chitosan/TPP and chitosan/TPP-hyaluronic acid nanoparticles: systematic optimisation of the preparative process and preliminary biological evaluation." *Pharmaceutical research* 26 (2009): 1918-1930. https://doi.org/10.1007/s11095-009-9908-0
15. Zhang, Hong, Megan Oh, Christine Allen, and Eugenia Kumacheva. "Monodisperse chitosan nanoparticles for mucosal drug delivery." *Biomacromolecules* 5, no. 6 (2004): 2461-2468. https://doi.org/10.1021/bm0496211
16. Desai, Kashappa Goud H., Susan R. Mallery, and Steven P. Schwendeman. "Effect of formulation parameters on 2-methoxyestradiol release from injectable cylindrical poly (DL-lactide-co-glycolide) implants." *European journal of pharmaceutics and biopharmaceutics* 70, no. 1 (2008): 187-198. https://doi.org/10.1016/j.ejpb.2008.03.007
17. Chen, Fu, Zhi-Rong Zhang, and Yuan Huang. "Evaluation and modification of N-trimethyl chitosan chloride nanoparticles as protein carriers." *International Journal of Pharmaceutics* 336, no. 1 (2007): 166-173. https://doi.org/10.1016/j.ijpharm.2006.11.027
18. Kafshgari, Morteza Hasanzadeh, Mohammad Khorram, Mobina Khodadoost, and Sahar Khavari. "Reinforcement of chitosan nanoparticles obtained by an ionic cross-linking process." *Iranian Polymer Journal* 20, no. 5 (2011): 445-456.
19. Nasti, Alessandro, Noha M. Zaki, Piero De Leonardis, Suwipa Ungphaiboon, Proramate Sansongsak, Maria Grazia Rimoli, and Nicola Tirelli. "Chitosan/TPP and chitosan/TPP-hyaluronic acid nanoparticles: systematic optimisation of the preparative process and preliminary biological evaluation." *Pharmaceutical research* 26 (2009): 1918-1930. https://doi.org/10.1007/s11095-009-9908-0

20. Bugnicourt, Loïc, and Catherine Ladavière. "Interests of chitosan nanoparticles ionically cross-linked with tripolyphosphate for biomedical applications." *Progress in polymer science* 60 (2016): 1-17. https://doi.org/10.1016/j.progpolymsci.2016.06.002
21. Agirre, Mireia, Jon Zarate, Edilberto Ojeda, Gustavo Puras, Jacques Desbrieres, and Jose LuisPedraz. "Low molecular weight chitosan (LMWC)-based polyplexes for pDNA delivery: from bench to bedside." *Polymers* 6, no. 6 (2014): 1727-1755. https://doi.org/10.3390/polym6061727
22. Chaudhury, Anumita, and Surajit Das. "Recent advancement of chitosan-based nanoparticles for oral controlled delivery of insulin and other therapeutic agents." *Aaps Pharmscitech* 12 (2011): 10-20. https://doi.org/10.1208/s12249-010-9561-2
23. Calvo, Pilar, Carmen Remuñan-López, Jose Luis Vila-Jato, and María José Alonso. "Chitosan and chitosan/ethylene oxide-propylene oxide block copolymer nanoparticles as novel carriers for proteins and vaccines." *Pharmaceutical research* 14 (1997): 1431-1436. https://doi.org/10.1023/A:1012128907225
24. El-Sayed, Ayman, Ikramy A. Khalil, Kentaro Kogure, Shiroh Futaki, and Hideyoshi Harashima. "Octaarginine-and octalysine-modified nanoparticles have different modes of endosomal escape." *Journal of Biological Chemistry* 283, no. 34 (2008): 23450-23461. https://doi.org/10.1074/jbc.M709387200
25. Rinaudo, Marguerite. "Chitin and chitosan: Properties and applications." *Progress in polymer science* 31, no. 7 (2006): 603-632. https://doi.org/10.1016/j.progpolymsci.2006.06.001
26. Xu, Yongmei, and Yumin Du. "Effect of molecular structure of chitosan on protein delivery properties of chitosan nanoparticles." *International journal of pharmaceutics* 250, no. 1 (2003): 215-226. https://doi.org/10.1016/S0378-5173(02)00548-3
27. Sai, Lin-Tao, Yong-Yuan Yao, Yan-Yan Guan, Li-Hua Shao, Rui-Ping Ma, and Li-Xian Ma. "Hepatitis B virus infection and replication in a new cell culture system established by fusing HepG2 cells with primary human hepatocytes." *Journal of Microbiology, Immunology and Infection* 49, no. 4 (2016): 471-476. https://doi.org/10.1016/j.jmii.2014.08.008
28. Flint, S. J., Racaniello, V. R., Romerio, A. M., and Shafer, P. "Principles of virology." (4th ed.). ASM Press. 2020.
29. Gripon, P., C. Diot, N. Theze, I. Fourel, O. Loreal, C. Brechot, and C. Guguen-Guillouzo. "Hepatitis B virus infection of adult human hepatocytes cultured in the presence of dimethyl sulfoxide." *Journal of virology* 62, no. 11 (1988): 4136-4143. https://doi.org/10.1128/jvi.62.11.4136-4143.1988
30. Lavie, Muriel, and Jean Dubuisson. "Interplay between hepatitis C virus and lipid metabolism during virus entry and assembly." *Biochimie* 141 (2017): 62-69. https://doi.org/10.1016/j.biochi.2017.06.009
31. Sanchez-Quant, Eva, Maria Lucia Richter, Maria Colomé-Tatché, and Celia Pilar Martinez-Jimenez. "Single-cell metabolic profiling reveals subgroups of primary human hepatocytes with heterogeneous responses to drug challenge." *Genome Biology* 24, no. 1 (2023): 234. https://doi.org/10.1186/s13059-023-03075-9
32. Felgner, Philip L., Thomas R. Gadek, Marilyn Holm, Richard Roman, Hardy W. Chan, Michael Wenz, Jeffrey P. Northrop, Gordon M. Ringold, and Mark Danielsen. "Lipofection: a highly efficient, lipid-mediated DNA-transfection procedure." *Proceedings of the National Academy of Sciences* 84, no. 21 (1987): 7413-7417. https://doi.org/10.1073/pnas.84.21.7413
33. Graham, Frank L., and Alex J. Van Der Eb. "A new technique for the assay of infectivity of human adenovirus 5 DNA." *virology* 52, no. 2 (1973): 456-467. https://doi.org/10.1016/0042-6822(73)90341-3
34. MacLaughlin, Fiona C., Russell J. Mumper, Jijun Wang, Jenna M. Tagliaferri, Inder Gill, Mike Hinchcliffe, and Alain P. Rolland. "Chitosan and depolymerized chitosan oligomers as condensing carriers for in vivo plasmid delivery." *Journal of controlled release* 56, no. 1-3 (1998): 259-272. https://doi.org/10.1016/S0168-3659(98)00097-2
35. Nallamothu, Ramakrishna, George C. Wood, Christopher B. Pattillo, Robert C. Scott, Mohammad F. Kiani, Bob M. Moore, and Laura A. Thoma. "A tumor vasculature targeted liposome delivery system for combretastatin A4: design, characterization, and in vitro evaluation." *Aaps Pharmscitech* 7 (2006): E7-E16. https://doi.org/10.1208/pt070232

36. Stewart, Martin P., Armon Sharei, Xiaoyun Ding, Gaurav Sahay, Robert Langer, and Klavs F. Jensen. "In vitro and ex vivo strategies for intracellular delivery." *Nature* 538, no. 7624 (2016): 183-192. https://doi.org/10.1038/nature19764
37. Shi, Baomin, Mengzhou Xue, Yi Wang, Yufeng Wang, Davey Li, Xiaomin Zhao, and Xinbo Li. "An improved method for increasing the efficiency of gene transfection and transduction." *International journal of physiology, pathophysiology and pharmacology* 10, no. 2 (2018): 95.
38. Kim, Tae Kyung, and James H. Eberwine. "Mammalian cell transfection: the present and the future." *Analytical and bioanalytical chemistry* 397 (2010): 3173-3178. https://doi.org/10.1007/s00216-010-3821-6
39. Fujii, Hodaka. "Receptor expression is essential for proliferation induced by dimerized Jak kinases." *Biochemical and biophysical research communications* 370, no. 4 (2008): 557-560. https://doi.org/10.1016/j.bbrc.2008.03.095
40. Mao, Shirui, Wei Sun, and Thomas Kissel. "Chitosan-based formulations for delivery of DNA and siRNA." *Advanced drug delivery reviews* 62, no. 1 (2010): 12-27. https://doi.org/10.1016/j.addr.2009.08.004
41. Ecker, Manuela, Gregory MI Redpath, Philip R. Nicovich, and Jérémie Rossy. "Quantitative visualization of endocytic trafficking through photoactivation of fluorescent proteins." *Molecular Biology of the Cell* 32, no. 9 (2021): 892-902. https://doi.org/10.1091/mbc.E20-10-0669
42. Ryu, WonHyoung, Sung Woo Min, Kyle E. Hammerick, Murty Vyakarnam, Ralph S. Greco, Fritz B. Prinz, and Rainer J. Fasching. "The construction of three-dimensional micro-fluidic scaffolds of biodegradable polymers by solvent vapor based bonding of micro-molded layers." *Biomaterials* 28, no. 6 (2007): 1174-1184. https://doi.org/10.1016/j.biomaterials.2006.11.002
43. Boussif, Otmane, Frank Lezoualc'h, MARLA ANTONIETrA Zanta, Mojgan Djavaheri Mergny, Daniel Scherman, Barbara Demeneix, and Jean-Paul Behr. "A versatile vector for gene and oligonucleotide transfer into cells in culture and in vivo: polyethylenimine." *Proceedings of the National Academy of Sciences* 92, no. 16 (1995): 7297-7301. https://doi.org/10.1073/pnas.92.16.7297
44. Richardson, SimonC W., HannoV J. Kolbe, and Ruth Duncan. "Potential of low molecular mass chitosan as a DNA delivery system: biocompatibility, body distribution and ability to complex and protect DNA." *International journal of pharmaceutics* 178, no. 2 (1999): 231-243. https://doi.org/10.1016/S0378-5173(98)00378-0